ELECTRIC POWER RESEARCH INSTITUTE

EPRI Flaw Growth and Flaw Tolerance Assessment for Dry Cask Storage Canisters

Shannon Chu
EPRI Nuclear Power Sector – High Level Waste Group

Kevin Fuhr
John Broussard
Glenn White
Dominion Engineering, Inc.

NRC Public Meeting with Nuclear Energy Institute on Material Degradation
August 5, 2014

Agenda

- Introduction
- Summary of Literature
  - References used to develop CGR model
- Crack Growth Rate Model
  - Approach and assumptions
  - CGR equation parameters
- Flaw Tolerance Assessment
  - Critical flaw size
  - Helium depressurization and air ingress
- Conclusions

Introduction - Background

- OE indicates that surface contamination by atmospheric chlorides combined with sufficient humidity and elevated stress can lead to CISCC of stainless steel
- Flaw growth and flaw tolerance assessment is part of industry effort to evaluate susceptibility to CISCC for stainless steel canisters and develop related aging management guidelines where needed
- Objectives
  - Develop quantitative model for CISCC growth
    - **Initiation will be considered separately in later work**
  - Determine limiting flaw sizes for canister structural tolerance
  - Calculate helium leak rate and air ingress rate for through-wall flaws

Introduction - Project Timeline

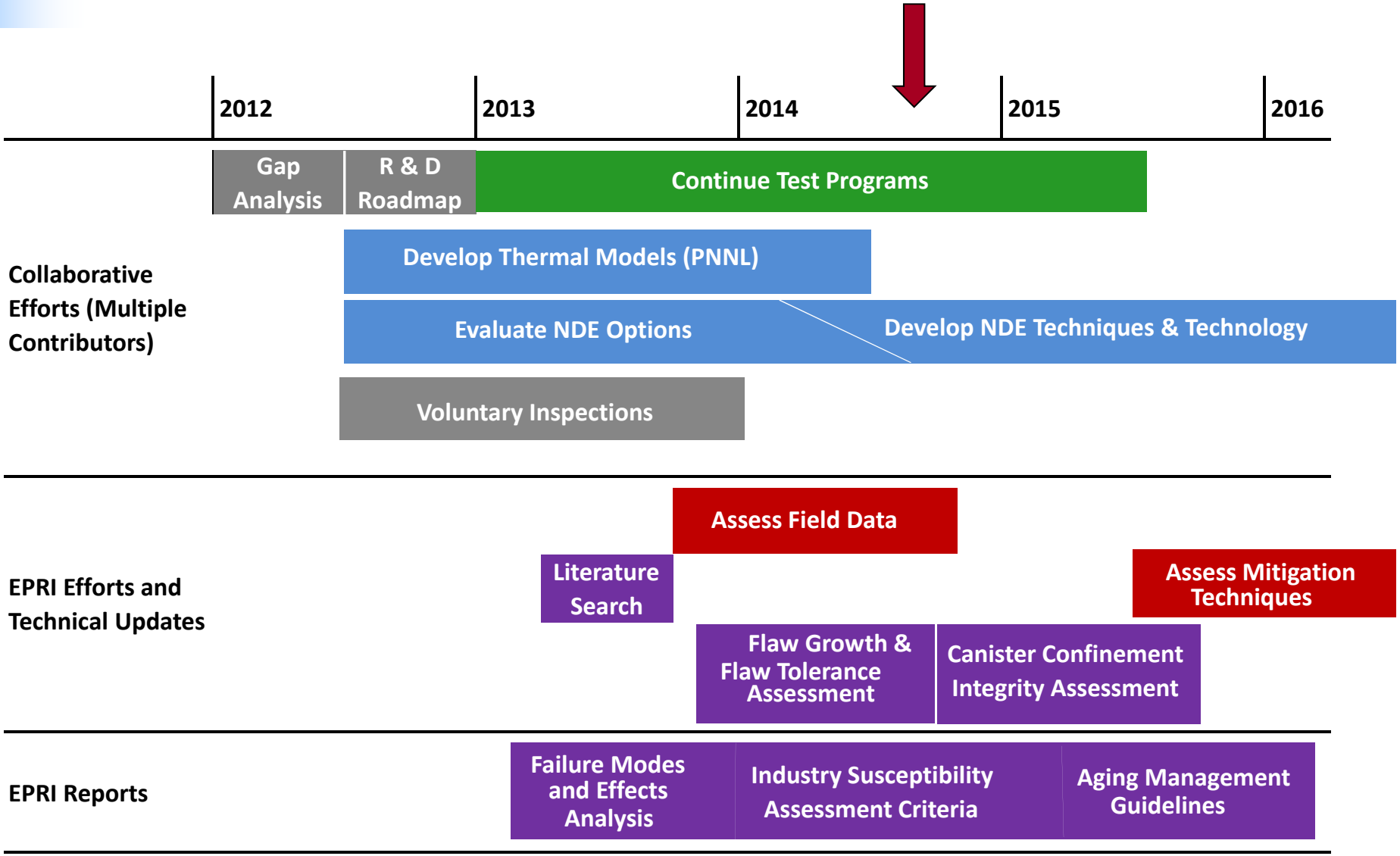

Introduction - Progression of Modeling

- Failure Modes and Effects Analysis
  - Qualitative judgments of frequency/probability, detectability, & severity over time based on literature and limited calculations
  - Define boundaries of the degradation problem & guide approach to subsequent assessments
- Canister Flaw Growth and Flaw Tolerance
  - Model flaw growth to thru-wall
  - Determine consequential flaw sizes
- Susceptibility Assessment Criteria
  - Model the process of canister degradation based on the pathways identified in the FMEA
- Canister Confinement Integrity Assessment
  - Probabilistic analysis to determine the benefit of various monitoring, mitigation, & inspection regimes

Introduction - Applications for Quantitative Model for CISCC Growth

- Model results will inform efforts to develop and demonstrate inspection technologies for identifying CISCC degradation in canisters
- Flaw growth model results can inform CISCC susceptibility criteria; these results do not include initiation probability or time to initiation which are key factors in susceptibility
  - Locations where flaw growth is expected to be slowest will be less susceptible
- Canister Confinement Integrity Assessment will build on flaw tolerance model results to provide technical basis for upcoming EPRI CISCC Aging Management Guidelines

Introduction - Applications for Quantitative Model for CISCC Growth

- Flaw growth model is a deterministic calculation that only considers time frame for flaw growth after initiation has occurred
- In many cases, significant amounts of time would be required to result in conditions leading to CISCC

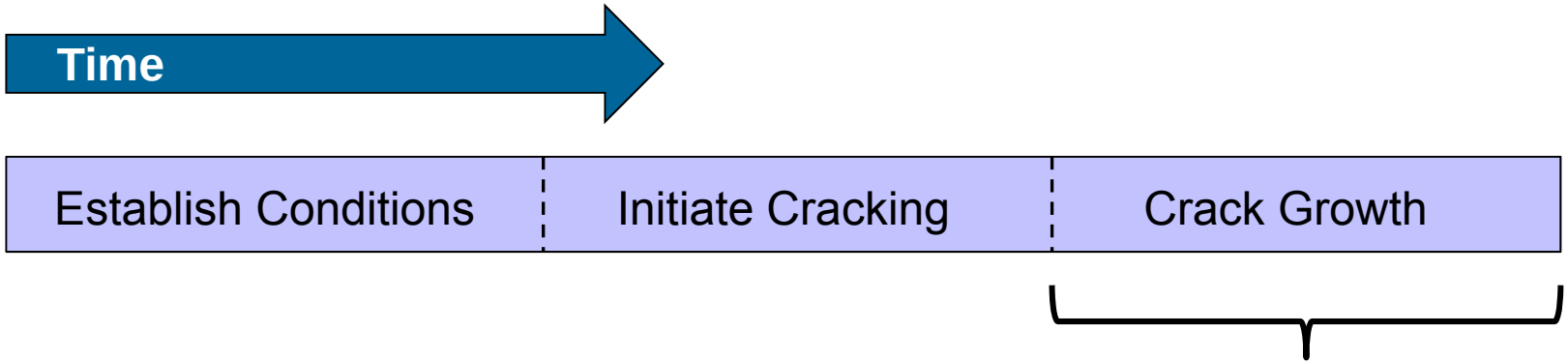

Summary of Literature Data

- Operating experience
- Key CISCC growth papers
- Prior approach to crack growth

Summary of Literature Data
Highlights

- There is plant operating experience of CISCC at marine locations
  - Different RH and airflow conditions from canisters
  - Cannot exclude potential for CISCC on canisters
- CRIEPI and Tani continuous crack growth monitoring show sharp change in crack growth rate at threshold depth
  - Likely mechanistic cause is particulates in partially deliquesced solution interfering with cathodic source at surface
- Crack growth rate generally observed to be dependent on temperature
- Crack growth rate generally observed no dependence on *K* value

Summary of Literature
Operating Experience

- CISCC on the OD of uninsulated piping and tanks at nuclear plants has been observed near ambient temperatures
  - San Onofre, Turkey Point, St. Lucie, Koeberg (S. Africa), Ohi (Japan), etc.
    - Plants essentially on the ocean and near breaking waves
      - Atmospheric source of chloride contamination
  - TW cracking observed on thinner (i.e., < 0.3 in) piping and components
    - In one instance TW cracking not observed on similar thicker piping in same location
  - Different RH and airflow conditions vs canisters in overpack
  - Cannot exclude potential for CISCC on canisters
- OE of CISCC due to other sources of chloride contamination not considered

Summary of Literature
Key CGR Paper – CRIEPI N10035 & Shirai 2011

- The CGR data in CRIEPI N10035 [1] (Japanese paper) is summarized in English in Shirai 2011 [1]
  - Not all data from N10035 is presented in Shirai
- Test Conditions
  - 10 mm thick, Type 304L, 4 pt. bending specimen with about 270 MPa at the surface; surface is sanded with 600 grit
  - 10 g/m^2 as Cl^- applied as a droplet of sea water
  - Specimens held at 35% RH and 80°C
- Reversing DC potential drop (DCPD) measurements used to continuously monitor crack depth
  - Calibration showed good linearity up to at least 2.5 mm deep

1. K. Shirai, J. Tani, and T Saegusa. *Study on Interim Storage of Spent Nuclear Fuel by Concrete Cask for Practical Use -Feasibility Study on Prevention of Chloride Induced Stress Corrosion Cracking for Type 304L Stainless Steel Canister*, CRIEPI N10035, 2011. (In Japanese)
2. K. Shirai, et al., "SCC Evaluation Test of a Multi-Purpose Canister," *International Conference on High Level Radioactive Waste Management*, Albuquerque, p. 824-831; Paper No. 3333, 2011.

Summary of Literature
Key CGR Paper – CRIEPI N10035 & Shirai 2011

- Crack propagation occurred in two phases (bi-linear transition)
  - Rapid growth through roughly the first 2 mm
  - Growth beyond this depth slower by a factor greater than 25

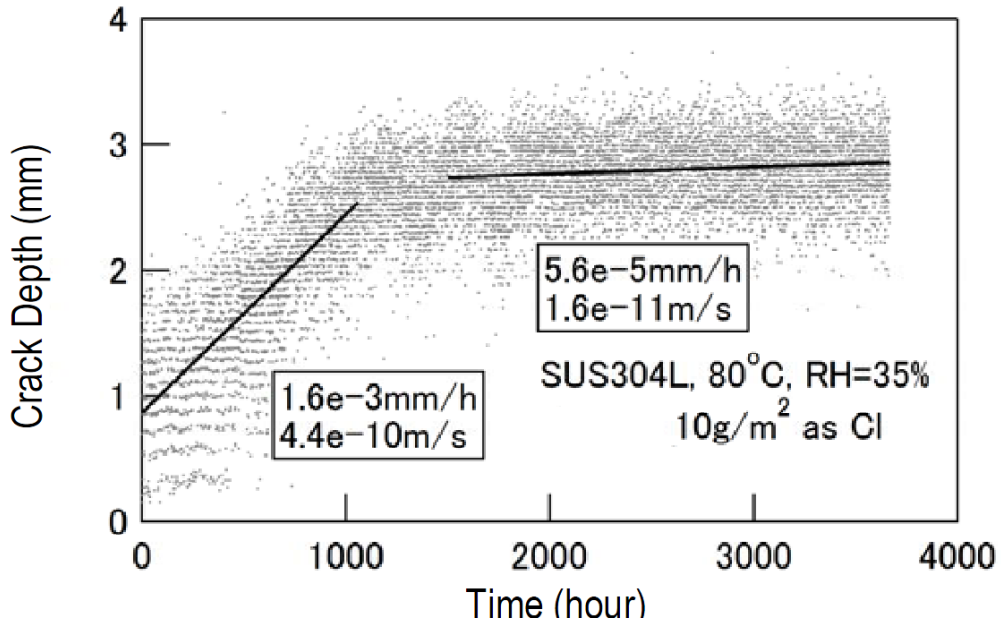

Figure Reprinted from Reference [1]

1. M. Wataru, "Japanese Current Status of Dry Storage and Aging Management Methodology and CRIEPI's Researches," Presentation at *Extended Storage Collaboration Program (ESCP)*, December 5, 2013.

Summary of Literature
Key CGR Paper – Tani 2009

- Test Conditions
  - Type 316L, CT specimens at crack-tip *K* between 5 and 30 MPa√m
  - Held at 35% RH and temperatures of 50°C and 80°C
  - Fatigue pre-crack
- Reversing DC potential drop measurements used to continuously monitor crack growth
- The data at 10-30 MPa√m were tightly grouped for each temperature
  - Factor of about 400 difference is consistent with an activation energy of 190 kJ/mol

1. J. I. Tani, "Initiation and Propagation of Stress Corrosion Cracking of Stainless Steel Canister for Concrete Cask Storage of Spent Nuclear Fuel," *Corrosion*, Vol. 65, No. 3, p. 187-194, 2009.

Summary of Literature
Key CGR Paper – Hayashibara 2008

- Test Conditions
  - 2 mm thick Type 304 tensile specimens
  - Held at 0.5-1.25 times the yield strength ($\sigma_{0.2\%}$= 313 MPa)
  - 35%, 55%, and 75% RH; 60°C, 70°C, and 80°C
- CGR measurement by measuring maximum crack length and depth at end of 120 hour test; no pre-cracks
- No SCC found for 75% RH; difference between RH of 35% and 55% explained as difference in initiation time
- Supports activation energies from 25-105 kJ/mol, with greatest support for 30-40 kJ/mol

1. H. Hayashibara, M. Mayuzumi, Y. Mizutani, J. Tani, “Effects of Temperature and Humidity on Atmospheric Stress Corrosion Cracking of 304 Stainless Steel,” *NACE Corrosion*, Paper 08492, 2008.

Summary of Literature
Key CGR Paper – Kosaki 2008

- Test Conditions (natural test)
  - Exposure to ambient climate at Miyakojima Island, Japan (severe marine site)
  - 3 pt. bending specimens of welded Type 304, 304L, and 316LN
    - Fatigue pre-cracked
  - Presented in terms of stress intensity (possibly calculated from the final crack size)
- Welds generally had lower CGR than base metal
- Different alloys exhibited similar CGR within the data scatter
- Natural data showed no *K* dependence within the scatter
- NaCl salt mist (accelerated test) data also indicates no *K* dependence

1. A. Kosaki, "Evaluation Method of Corrosion Lifetime of Conventional Stainless Steel Canister under Oceanic Air Environment," *Nuclear Engineering and Design,* Vol. 238, No. 5, p. 1233–1240, 2008.

Summary of Literature
Deliquescence Behavior

- Corrosion of stainless steel by chloride salts occurs above the deliquescent relative humidity (DRH), the RH where salt dissolves in absorbed water, but limited corrosion may occur from absorbed film on salt particles slightly below the DRH[1]
- DRH of sea salt is comparable to, or slightly less than, the DRH of $MgCl_2$[2]
  - Sea salt does not fully deliquesce until RH approaches DRH of NaCl (RH ~ 75%)
- Hysteresis occurs for RH between the DRH and ERH[2]
- Data combining initiation and growth indicate co-dependence on RH and salt loading varies over the range of possible values

1. M. Mayuzumi, J. Tani, and T. Arai, “Chloride-induced stress corrosion cracking of candidate canister materials for dry storage of spent fuel,” *Nuclear Engineering and Design*, Vol. 238, p. 1227–1232, 2008.
2. X. He, T.S. Mintz, R. Pabalan, L. Miller, and G. Oberson, *Assessment of Stress Corrosion Cracking Susceptibility for Austenitic Stainless Steels Exposed to Atmospheric Chloride and Non-Chloride Salts,* Southwest Research Institute, NUREG/CR-7170, February 2014.

Summary of Literature
Discussion of CGR vs Depth

- CRIEPI DCPD testing indicates that the propagation rate may be most rapid during the initial few mm of penetration[1]
  - Testing by Tani also using DCPD also appears to slow after propagating 2 mm beyond the pre-crack
  - Other testing performed with specimens < 2 mm thick or resulted in cracks less than 2 mm deep
- CRIEPI testing observed the dependence of CGR with depth was inconsistent with a *K* dependence
  - Sharp transition between two constant growth rates

1. K. Shirai, J. Tani, and T Saegusa. *Study on Interim Storage of Spent Nuclear Fuel by Concrete Cask for Practical Use -Feasibility Study on Prevention of Chloride Induced Stress Corrosion Cracking for Type 304L Stainless Steel Canister*, CRIEPI N10035, 2011. (In Japanese)

Summary of Literature
Discussion of CGR vs Depth

- Mechanistic cause may be the presence of particulates in the electrolyte layer reduces the cathode capacity through (1) increased ohmic resistance, (2) interrupting the cathode continuity, and (3) impeding the transport of oxygen[1]
- Increased resistance with crack depth results in a limited cathodic capacity that reduces crack growth after a threshold depth
- Crack in CRIEPI specimen doped with $MgCl_2$ grew to about 4 mm with only a slight decrease in rate at 3.5 mm
  - Same RH, T, and [Cl^-] as sea salt tests
  - Different behavior due to full deliquescence of $MgCl_2$ vs partial deliquescence of sea salt at test conditions

1. R.G. Kelly, et al., "Considerations of the Role of the Cathodic Region in Localized Corrosion" Yucca Mountain Project, U.S. Department of Energy, March 17, 2006.

Flaw Growth Assessment

- Modeling approach
- CGR model assumptions and dependencies
- Assessments of CGR dependence from literature data

Flaw Growth
Modeling Approach

- Assessment considers CISCC; through-wall penetration by pitting/crevice corrosion in atmosphere considered much less likely based on literature review and FMEA
- Deterministic calculation of potential flaw growth rates
  - Prior crack initiation is assumed for the flaw growth calculation
  - CISCC initiation not readily treated in a deterministic framework
- Cracks in the canister shell near welds are most likely to occur and to penetrate the pressure boundary first

Flaw Growth
Modeling Approach – Form of CGR Equation

$$\frac{da}{dt} = \alpha \left(K_I - K_{I\text{th}} \right)^n f_T f_H f_S$$

- Based on typical form of SCC growth equations with factors based on empirical data to account for dependences
  - E.g., ASME BPVC Section XI, Article C-8500
- Primarily an empirical model that fits available data to expected dependences on environmental factors

Where:

- α = CGR coefficient
- K_I = Stress intensity factor
- $K_{I\text{th}}$ = *K* threshold
- n = *K* exponent
- f_T = Arrhenius temperature factor
- f_H = Humidity factor
- f_S = Salt/Chloride factor

Flaw Growth
Effective CGR Equation

$$\frac{da}{dt} = \begin{cases} \alpha \exp\left[-\frac{Q_g}{R}\left(\frac{1}{T}-\frac{1}{T_{ref}}\right)\right] & \text{for } RH \geq DRH \text{ and } K_I > 0 \\ 0 & \text{for } RH < DRH \text{ or } K_I \leq 0 \end{cases}$$

$$\text{where} \quad \alpha = \begin{cases} \alpha_{shallow} & \text{for } a < a_{trans} \\ \alpha_{deep} & \text{for } a \geq a_{trans} \end{cases}$$

- CGR parameters based on substantial statistical conservatism
  - a_{trans} = 3.2 mm
  - $\alpha_{shallow}$ = 168 mm/yr (at 80°C T_{ref}) → 74.1 mm/yr at 60°C
  - α_{deep} = 2.2 mm/yr (at 80°C T_{ref}) → 0.97 mm/yr at 60°C
- Activation energy taken to be 40 kJ/mol (T_{ref}= 80°C)
  - Among supportable Q_g, the low choice is conservative
- Threshold RH for growth is a conservatively low effective DRH, 7% RH lower than that of $MgCl_2$
  - Bounds measured Efflorescent Relative Humidity (ERH) values in NUREG/CR-7170

Flaw Growth
Modeling Approach – CGR Coefficient α

- Data used to determine CGR coefficient limited to most relevant experimental conditions
  - Data combining initiation plus growth not included
  - Atmospheric data subject to uncertain environment (e.g., solar heating) not included
  - Only data using sea salt exposure is included
- Most severe canister environment expected to be at marine sites with sea salt as the predominant source of chloride
  - Exposure will be to multi-component salts and mixture of deliquescent and insoluble particles, not a fully deliquesced salt

Flaw Growth
Modeling Approach – CGR Coefficient α

- CRIEPI sea salt exposure CGR data previously noted to have observed two growth rates, one for shallow flaw growth and one for deep flaw growth
- Two CGR coefficients developed: one for shallow flaw growth and one for deep crack growth
  - CGR coefficient data set includes CRIEPI and Tani data
- Depth at which transition occurs also developed based on CRIEPI data
- Data normalized to 80°C reference temperature; most data already performed at this temperature

Flaw Growth
Modeling Approach – CGR Coefficient α

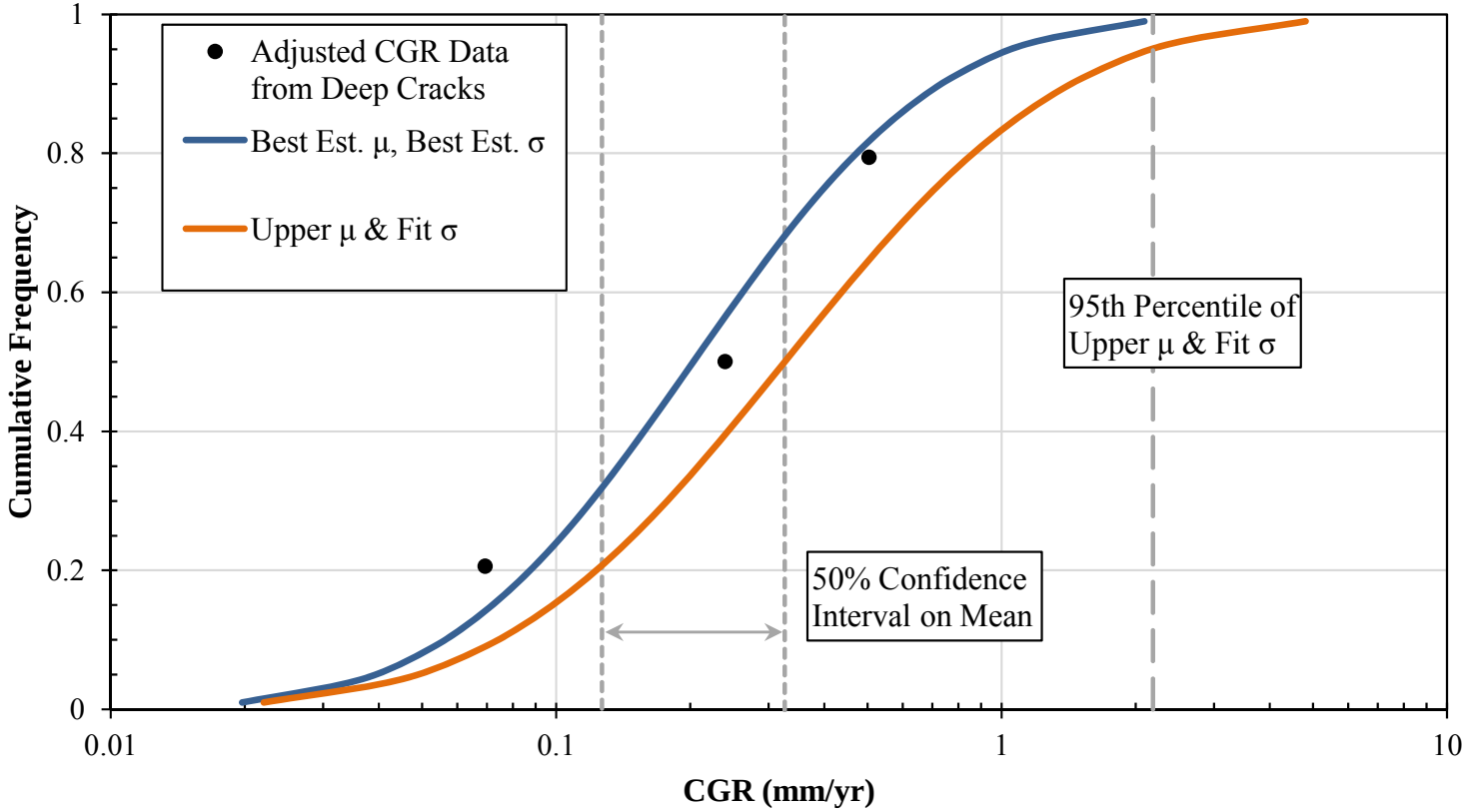

- Statistical approach for deep flaw CGR coefficient shown as example
- Same approach used for shallow CGR coefficient and for transition depth

Flaw Growth
Modeling Approach – CGR Coefficient α

- Small set of available data requires careful statistical treatment to determine appropriately conservative values for deterministic calculations
- Approach considers additional uncertainty associated with small data set
  - Standard statistical methods used calculate the best estimate for the mean (μ) and the standard deviation (σ) in small data set
  - A new, higher mean value (*upper* μ) is calculated using a 50% confidence interval
    - Value is the 75th percentile of the distribution of mean values
  - A new standard deviation (*fit* σ) is fit to the data using *upper* μ as the true mean of the distribution
- The CGR coefficient is calculated as the 95th percentile of the distribution defined by the *upper* μ mean and the *fit* σ standard deviation
- The resulting CGR coefficient values are therefore based on substantial statistical conservatism

Flaw Growth
Modeling Approach – K Dependence $(K_I\text{-}K_{Ith})^n$

- Minimal evidence in literature of threshold K_{Ith} value for atmospheric CISCC
  - Conservatively assumed to be 0
- Power law dependence on K appears weak and generally lost within data scatter[1] (n = 0)
- In testing using CT specimens from 5-30 MPa√m, only the 5 MPa√m point showed a different CGR[2]
  - Corroborates the lack of dependence in Reference [1]

1. A. Kosaki, "Evaluation Method of Corrosion Lifetime of Conventional Stainless Steel Canister under Oceanic Air Environment," *Nuclear Engineering and Design,* Vol. 238, No. 5, p. 1233–1240. 2008.
2. J. I. Tani, "Initiation and Propagation of Stress Corrosion Cracking of Stainless Steel Canister for Concrete Cask Storage of Spent Nuclear Fuel," *Corrosion*, Vol. 65, No. 3, p. 187-194, 2009.

Flaw Growth
Stress Intensity Factor

- Flaw initiation still stress dependent and is most likely to occur in weld regions
- Cracks more likely to be oriented perpendicular to direction of principal stress, i.e. transverse to the weld

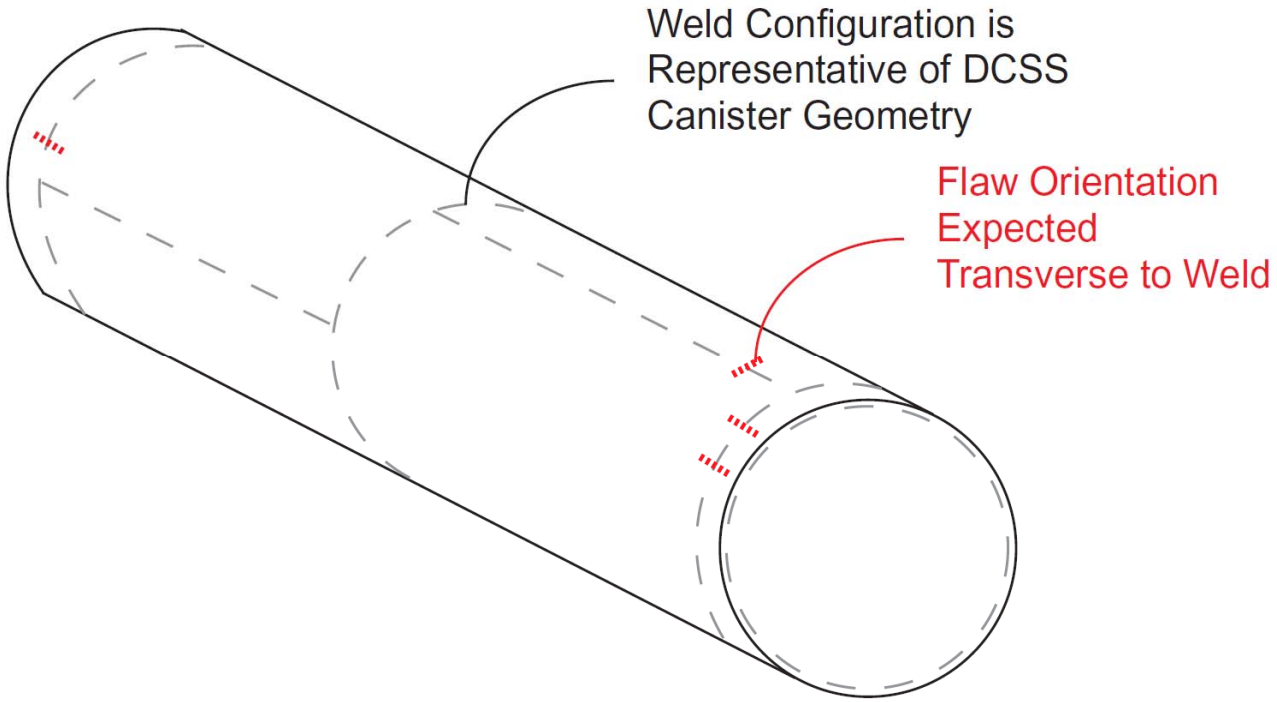

Flaw Growth
Modeling Approach – Temperature Dependence f_T

- Arrhenius relation dependence on temperature
- Activation energy used to normalize available data to a reference temperature
  - Choice of reference temperature does not matter if data is re-fit each time
- Crack growth testing typically shows a strong dependence on temperature
  - Reported strength of dependence (value of activation energy, Q_g) varies widely from about 25 to 190 kJ/mol[1],[2],[3]
- Strong support for Q_g of 30-40 kJ/mol and reasonable support for about 80 kJ/mol[1],[3]

1. K. Shirai, et al., "Research on Spent Fuel Storage and Transportation in CRIEPI (Part 2 Concrete Cask Storage)," *16th Pacific Basin Nuclear Conference (16PBNC)* held in Aomori, Japan, Paper No. P16P1215, October 13-18, 2008.
2. J. I. Tani, "Initiation and Propagation of Stress Corrosion Cracking of Stainless Steel Canister for Concrete Cask Storage of Spent Nuclear Fuel," *Corrosion*, Vol. 65, No. 3, p. 187-194, 2009.
3. H. Hayashibara, M. Mayuzumi, Y. Mizutani, J. Tani, "Effects of Temperature and Humidity on Atmospheric Stress Corrosion Cracking of 304 Stainless Steel," *NACE Corrosion*, Paper 08492, 2008.

Flaw Growth
Modeling Approach – Humidity Dependence f_H

- Crack growth is modeled to occur only when RH (based on surface temperature and ambient AH) is greater than effective DRH
- Effective DRH chosen to be conservatively low
  - Bounds the lower ERH values in NUREG/CR-7170
  - Eliminates need to model hysteresis between DRH and ERH, drying time, etc.
- Temperature dependence assumed to parallel that of $MgCl_2$ (but set 7% RH lower)
  - Consistent with available DRH/ERH data and CISCC initiation testing (accounting for potential for CISCC in partial deliquescence)

Flaw Growth
Modeling Approach – Humidity Dependence f_H

- Above DRH, no definitive dependence of crack growth on DRH
  - Hayashibara did not report difference in growth rate at 35% and 55%
  - Albores-Silva reported conflicting dependences on RH at different salt loadings

1. H. Hayashibara, M. Mayuzumi, Y. Mizutani, J. Tani, “Effects of Temperature and Humidity on Atmospheric Stress Corrosion Cracking of 304 Stainless Steel,” *NACE Corrosion*, Paper 08492, 2008.
2. O. E. Albores-Silva, E. A. Charles, and C. Padovani, “Effect of Chloride Deposition on Stress Corrosion Cracking of 316L Stainless Steel Used for Intermediate Level Radioactive Waste Containers,” *Corrosion Engineering,* Vol. 46, No. 2, 2011.

Combined Treatment of Temperature and Humidity ($f_T f_H$)

- The canister surface temperature is directly influenced by the ambient temperature
- Ambient temperature and ambient humidity data are available from climate monitoring locations
- Temperature and humidity data may be combined to generate piecewise crack growth vs time

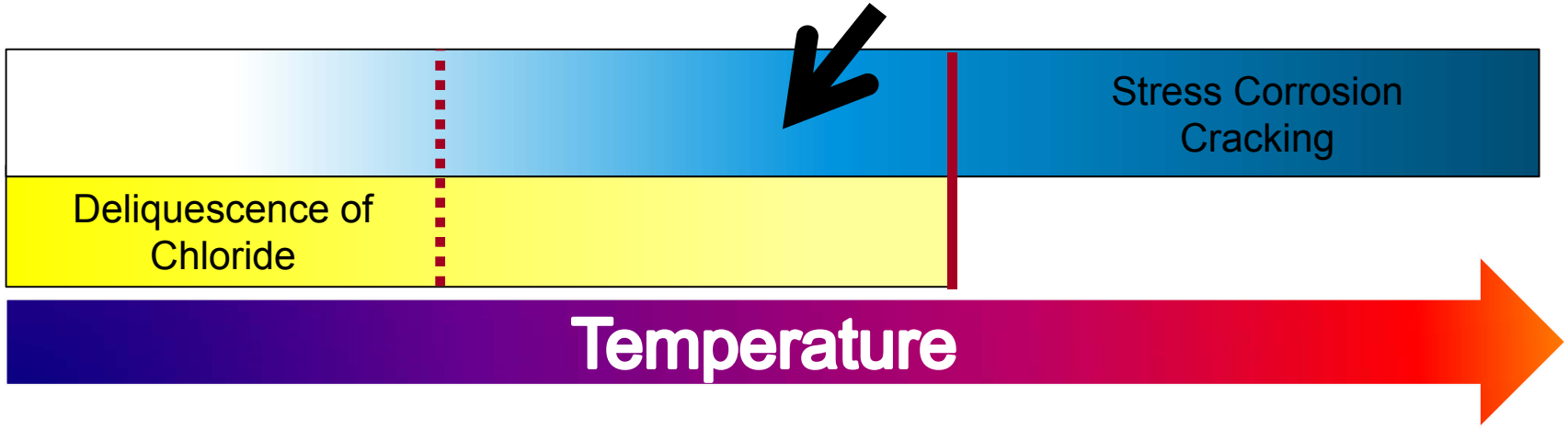

Flaw Growth
Modeling Approach – Other Dependencies

- Available data doesn't support salt loading factor in CGR (f_s)
  - Data includes initiation time and shows conflicting correlations with salt load
  - CGR coefficient based on experiments using high salt loadings (~10 g/m^2) – likely bounding
- Laboratory testing using Types 316L, 304L, and 304 did not demonstrate substantial CGR differences among alloys[1]
  - Type 316 and low-carbon variants are less susceptible in initiation testing
- Initiation and growth data shows that weld metal is less susceptible than base metal

1. A. Kosaki, "Evaluation Method of Corrosion Lifetime of Conventional Stainless Steel Canister under Oceanic Air Environment," *Nuclear Engineering and Design,* Vol. 238, No. 5, p. 1233–1240. 2008.

Flaw Tolerance Assessment

- Critical Flaw Size
- Helium Depressurization
- Air Ingress

Critical Flaw Size
Approach

- Calculated using limit load criterion
  - Use ASME BPVC Section XI, Article C-5000 method (fully plastic limit load evaluation)
  - Applicable for austenitic base materials
- Load cases taken from design basis values
  - Normal case with pressure and handling loads
  - Accident case with accident pressure and normal handling

Critical Flaw Size
Evaluation Cases

- Part-depth (PD) flaw cases postulate an arbitrarily long axial or full circumference crack
  - Limiting case for considering multiple flaw initiation
- Through-wall (TW) cases represent a flaw with a thin ligament remaining before going TW
- Designs evaluated: NUHOMS 32PT, HI-STORM 24, NAC-UMS PWR, and MAGNASTOR PWR
- Example results for Hi-Storm 24
  - Normal load case, Max TW Axial (crack across girth weld) is 1.2 m = 25% of the canister length
  - Normal load case, Max TW Circ (crack across seam weld) is 3.3 m = 60% of canister circumference
- **All cases show canister is highly flaw tolerant (leak before break)**

Internal Gasses
Approach

- Leak rate solved to result in pressure losses which balance the pressure differential
  - Viscous, entrance, exit, and tortuosity pressure losses
- Crack opening displacements expected to be smaller than calculated using simplified model based on idealized geometry
  - Reference indicates that 16-30 μm opening are likely for SCC cracks
  - Simplified model calculates 130 μm opening; WRS provides most of the opening force
- Pressure and moles of helium tracked within the canister free volume

Internal Gasses
Helium Depressurization

- Start at design normal pressure (a conservative approach)
  - After decades of storage, the expected pressure would be much lower
  - Conservative for leak rate
- Graph shown is for tight flaw (25 mm x 20 µm) and high initial pressure (100 psi)
- Depressurization time is negligible on time scale of extended storage
- Insensitive to assumed internal gas temperature, most sensitive to the crack opening size

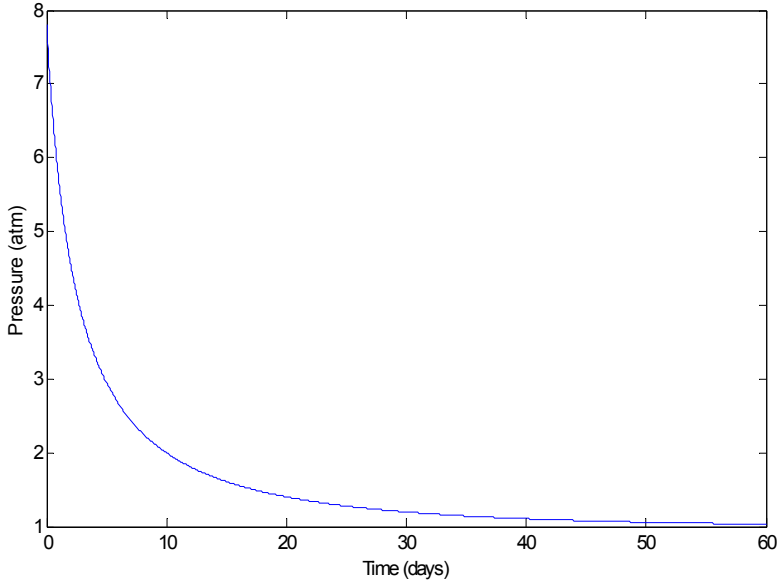

Internal Gasses
Air Ingress

- Caused by internal gas expansion/contraction with ambient pressure and temperature variation
- Cases evaluated with idealized inputs and with actual atmospheric data
- Graph at right is for tight flaw (25 mm x 20 μm) and a year's climate data
- Wider cracks are insensitive to canister and flaw geometry, but occur much faster
  - Limited by fluctuation of pressure and temperature instead of leak rate

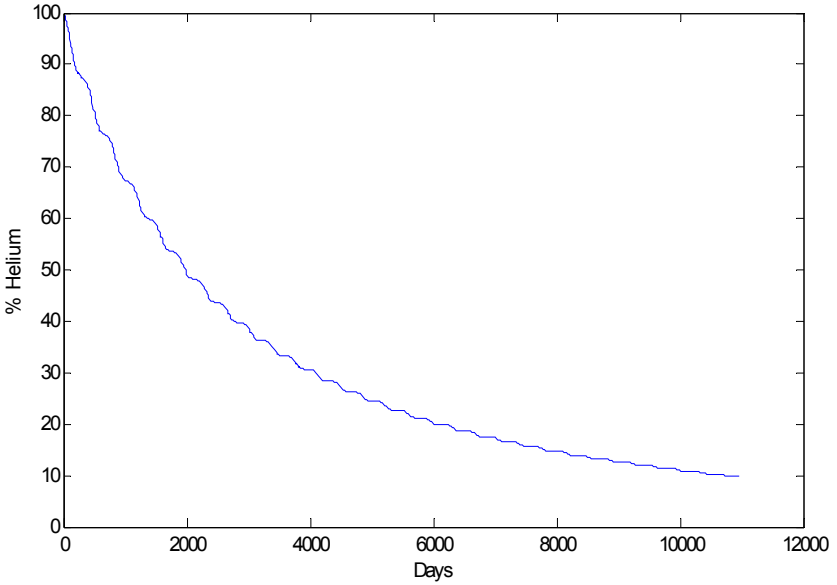

Conclusions

Conclusions

- Crack growth was modeled independent of crack initiation
- Crack growth model based on most relevant data
  - Substantial statistical conservatism applied to data in consideration of limited data set
- Available data does not support crack growth rate dependence on SS material alloy, degree of salt loading, or crack *K* value
  - Model assumes initiation has occurred due to the presence of these factors
  - Model conservatively assumes unity for material alloy and salt loading dependence
- Crack growth rate equation models dependence on temperature and humidity

Conclusions

- Canisters are highly flaw tolerant under typical loads and under accident pressure
- Depressurization is likely to be relatively rapid compared to other steps (from establishment of conditions to air ingress)
  - Backfill pressure will be closer to ambient than design normal pressure at time of leak due to decay of thermal power
- Air ingress will take much longer (likely years) to replace most of the helium than depressurization time
  - "Breathing" mechanism is more rapid than diffusion

Future Deliverables

- Susceptibility Assessment Criteria
  - Criteria to assess ISFSI environment
  - Criteria to assess individual canisters at an ISFSI
- Probabilistic assessment of flaw growth and tolerance
  - To include modeling of periodic canister inspections
- Aging Management Guidelines

Together…Shaping the Future of Electricity